On Evolute Cusps and Skeleton Bifurcations

Alexander Belyaev and Shin Yoshizawa

The University of Aizu

Aizu-Wakamatsu 965-8580 Japan

{belyaev, m5031126}@u-aizu.ac.jp

Abstract

Consider a 2D smooth closed curve evolving in time, the skeleton (medial axis) of the figure bounded by the curve, and the evolute of the curve. A new branch of the skeleton can appear/disappear when an evolute cusp intersects the skeleton. In this paper, we describe exact conditions of the skeleton bifurcations corresponding to such intersections. Similar results are also obtained for 3D surfaces evolving in time.

Introduction

The *skeleton* or *medial axis* of a planar figure is the closure of the set of centers of maximal disks contained inside the figure, i.e., those discs contained in the figure but in no other disc in the figure. The skeleton is an important shape descriptor invented by Blum [6]. It is extensively used in connection with human shape perception theories [5], [9]. Fig. 1 shows simple closed curves mimicking silhouettes of a bison, a fish, and a human and their skeletons.

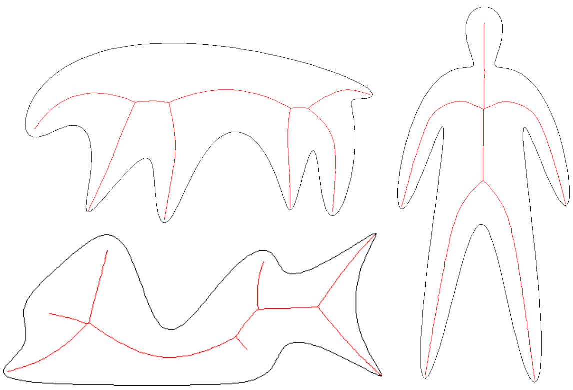

Figure 1. Simple closed curves mimicking silhouettes of a bison, a fish, and a human and their skeletons.

Fig. 2 demonstrates the description of the skeleton of a figure as the set of centers of maximal disks inscribed in the figure.

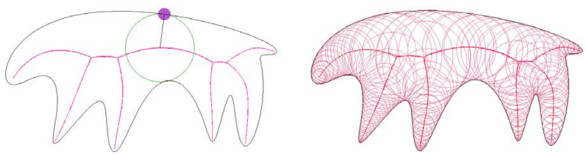

Figure 2. Left: a "bison" figure, its skeleton, and a maximal disk inscribed in the figure; the bold point is a point of tangency betw een the disk and the boundary of the figure. Right: the skeleton of a figure can be defined as the set of centers of maximal disks inscribed in the figure.

Consider a figure evolving in time. How does the skeleton of the figure change? An analytical description of how smooth points of the skeleton evolve under a general boundary evolution is given in [1] for the 2D case. This paper addresses conditions of topological changes of the skeleton. Fig. 3 demonstrates two topological changes of the skeleton of an evolving curve: in the "head" and in the "chest". In this paper, we deal with the skeleton bifurcations similar to the bifurcation happened in the "head" where a new skeleton branch has grown from an inner point of the skeleton.

Let us recall that the best approximation of a curve at its point P by a circle is given by the *circle of curvature* called also the *osculating circle* at P [12]. If P is an inflection point (where the curvature is zero), the circle of curvature degenerates into the tangent line at P. The locus of the centers of curvature of a given curve is called the *evolute* of the curve. The evolute of a smooth curve has singularities (so-called cusps).

A rigorous mathematical description of the relations between the skeleton and the evolute (the focal surface in 3D) of a simple closed curve (a simple closed surface in 3D) evolving in time constitutes the main results of the paper.

The 2D version of the skeleton branching theorem de-

Proceedings of the International Conference on Shape Modeling and Applications (SMI '01)
0-7695-0853-7/01 $10.00 © 2001 IEEE

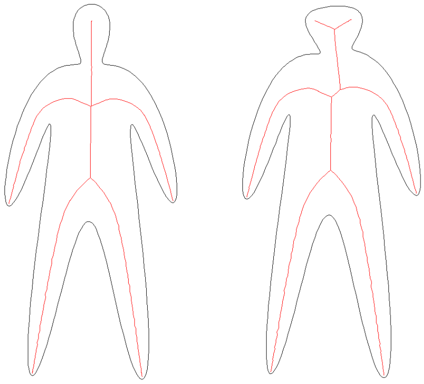

Figure 3. Two different skeleton bifurcations happened in the "head" and in the "chest". In the "head" the new skeleton branch has grown from an inner point of the skeleton.

scribed in the next section was discovered while playing with the Java 2D Curve Simulator [1] described in [14].

2D Skeleton Branching Theorem

Let us consider a planar curve $\mathbf{r} = \mathbf{r}(s)$ parameterized by arc length s. To study the shape of the evolute of the curve at a small vicinity of a point $\mathbf{r}(s)$ we expand $\mathbf{r}(s+\alpha)$ into Taylor series with respect to α, $\alpha \ll 1$. Let

$$\mathbf{r}' = \mathbf{t} \quad \text{and} \quad \mathbf{n} = \mathbf{t}^{\perp}$$

compose the Frenet frame at $\mathbf{r} = \mathbf{r}(s)$. The evolute is given by

$$\mathbf{e}(s) = \mathbf{r}(s) + \frac{\mathbf{n}(s)}{k(s)},$$

where $k(s)$ is the curvature of the curve at $\mathbf{r}(s)$. According to the Frenet formulas

$$\mathbf{t}' = k\,\mathbf{n}, \quad \mathbf{n}' = -k\,\mathbf{t}$$

we have

$$\mathbf{r}' = \mathbf{t}, \qquad \mathbf{r}'' = \mathbf{t}' = k\,\mathbf{n}, \qquad \mathbf{r}''' = (k\mathbf{n})' = k'\mathbf{n} - k^2\mathbf{t}.$$

It yields

$$\begin{aligned}\mathbf{r}(s+\alpha) &= \mathbf{r} + \alpha\mathbf{r}' + \frac{\alpha^2}{2}\mathbf{r}'' + \frac{\alpha^3}{6}\mathbf{r}''' + O\left(\alpha^4\right) = \\ &= \mathbf{r}(s) + \mathbf{t}\left[\alpha - \frac{\alpha^3}{6}k^2 + O\left(\alpha^4\right)\right] + \\ &\quad + \mathbf{n}\left[\frac{\alpha^2}{2}k + \frac{\alpha^3}{6}k' + O\left(\alpha^4\right)\right].\end{aligned}$$

[1] http://www.u-aizu.ac.jp/~m5031126/Research/CCurve/CCurve.html

Similarly,

$$\begin{aligned}\mathbf{n}' &= -k\mathbf{t}, \\ \mathbf{n}'' &= (-k\mathbf{t})' = -k'\mathbf{t} - k^2\mathbf{n}, \\ \mathbf{n}''' &= (-k'' + k^3)\,\mathbf{t} - 3k'k\,\mathbf{n},\end{aligned}$$

$$\begin{aligned}\mathbf{n}(s+\alpha) &= \mathbf{n}(s) + \\ &+ \mathbf{t}\left[-\alpha\,k - \frac{\alpha^2}{2}k' + \frac{\alpha^3}{6}\left(k^3 - k''\right) + O(\alpha^4)\right] + \\ &+ \mathbf{n}\left[-\frac{\alpha^2}{2}k^2 - \frac{\alpha^3}{2}kk' + O(\alpha^4)\right],\end{aligned}$$

$$k(s+\alpha) = k(s) + \alpha\,k' + \frac{\alpha^2}{2}k'' + O(\alpha^3),$$

$$\frac{1}{k(s+\alpha)} = \frac{1}{k(s)} - \alpha\,\frac{k'}{k^2} + \alpha^2\left(\frac{k'^2}{k^3} - \frac{k''}{2k^2}\right) + O(\alpha^3).$$

For the evolute point $\mathbf{e}(s+\alpha)$ we have

$$\begin{aligned}\mathbf{e}(s+\alpha) &= \mathbf{r}(s+\alpha) + \frac{\mathbf{n}(s+\alpha)}{k(s+\alpha)} = \mathbf{e}(s) + \\ &+ \mathbf{t}\left[\alpha^2\frac{k'}{2k} + \alpha^3\left(\frac{k''}{3k} - \frac{k'^2}{2k^2}\right) + O(\alpha^4)\right] + \\ &+ \mathbf{n}\left[-\alpha\,\frac{k'}{k^2} + \alpha^2\left(\frac{k'^2}{k^3} - \frac{k''}{2k^2}\right) + O(\alpha^3)\right]\end{aligned} \tag{1}$$

Thus, if $k'(s) \neq 0$, in a small vicinity of the center of curvature $\mathbf{r}(s) + \mathbf{n}(s)/k(s)$ the evolute is approximated by a parabola tangent to the normal $\mathbf{n}(s)$ (see the left image of Fig. 4). If $k'(s) = 0$ then (1) simplifies into

$$\begin{aligned}&\mathbf{e}(s+\alpha) - \mathbf{e}(s) = \\ &= \mathbf{t}\left[\alpha^3\frac{k''}{3k} + O(\alpha^4)\right] + \mathbf{n}\left[-\alpha^2\frac{k''}{2k^2} + O(\alpha^3)\right].\end{aligned} \tag{2}$$

For a generic curve k' and k'' do not vanish simultaneously. Thus, in a small vicinity of the center of curvature, the evolute is approximated by a semicubic parabola $y^3 = Ax^2$ tangent to the normal $\mathbf{n}(s)$. See the middle and right images of Fig. 4.

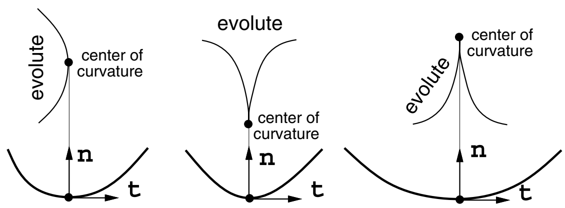

Figure 4.

A *vertex* of a smooth curve is a point of the curve where the curvature takes an extremal value, $k' = 0$.

Proposition 1 *The evolute of a curve* $\mathbf{r}(t)$ *has a cusp at* t_0 *if and only if* $\mathbf{r}(t_0)$ *is a vertex of the curve. The cusp on the evolute is pointing towards or away from the vertex according as the absolute value of the curvature has a local minimum or maximum at* t_0*.*

Now the proposition follows immediately from (2). A different proof can be found in [10].

For a generic curve, the osculating circles centered at ordinary evolute points intersect the curve. The osculating circles centered at the cusps of the evolute have either inner or outer contacts with the curve. The previous proposition can be reformulated as follows.

Proposition 2 *Given a generic curve, the osculating circle centered at an evolute cusp pointing towards (away from) the curve has an inner (outer) contact with the curve.*

The circle of curvature centered at a skeleton endpoint can be considered as a limit of the inner bitanget circles (i.e., touching the curve at least twice) whose centers form the skeleton. Thus the circle is osculating and it has an inner contact with the boundary of the figure. If the boundary of the figure is oriented by its inner normal, the endpoints of the skeleton correspond to positive maxima of the curvature of the boundary and we arrive at the following result.

Proposition 3 *The endpoints of the skeleton of a figure are located at cusps of the evolute of the boundary of the figure. Those cusps are pointing towards the boundary of the figure.*

However the evolute cusps do not necessary coincide with the endpoints of the skeleton of the figure bounded by the curve. If the osculating circle centered at a cusp of the evolute does not lie inside the figure, then the cusp is not a skeleton endpoint. Fig. 5 suggests the following result.

Theorem 1 *Given a generic closed curve, consider the segment connecting an evolute cusp and its associated curve vertex. The cusp is an endpoint of the skeleton if and only if the segment does not intersect the skeleton.*

Before proving the theorem we need the following result.

Proposition 4 *An inner circle of a generic closed curve has a high-order contact with the curve if and only if the circle center is a skeleton endpoint.*

Following [7] consider the family of distance-squared functions

$$\mathrm{dist}_Q^2(P) = \|P - Q\|^2,$$

where P lies on the curve and Q lies inside the curve, Q parameterizes the family. It can be shown, see, for example, [7], that Q lies on the evolute if and only if its distance-squared function has a degenerate critical point. It is easy

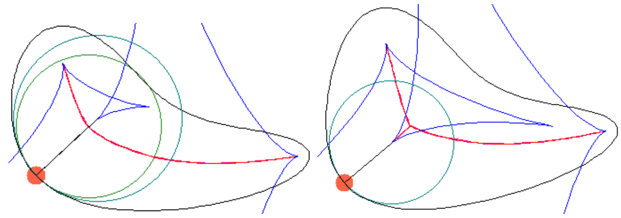

Figure 5. Left: A closed curve; its skeleton and evolute; an osculating circle centered at a cusp of the evolute and its radial segment connecting the cusp and the tangency point; an inner bitangent circle touching the curve at the same point as the osculating circle does and, therefore, contained by the osculating circle. Right: the curve is modified such that the radial segment connecting the cusp and the tangency point intersects the skeleton; note appearance of a new skeleton branch ended at the cusp.

to see that the function has two equal absolute minima if and only if Q is a generic point of the skeleton of the figure bounded by the curve. Let us move Q along the skeleton towards a skeleton endpoint. A degenerate absolute minimum appears when Q reaches the endpoint and the absolute minima merge. See Fig. 6. An inner circle has a high-order contact with the curve if and only if the distance-squared function with Q located at the center of the circle has a degenerate absolute minimum. This proves the proposition.

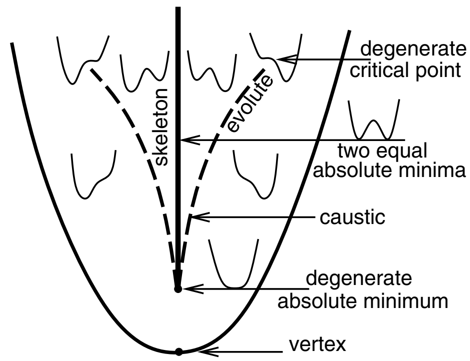

Figure 6. Zoo of distance functions.

PROOF OF THEOREM 1. If the segment crosses the skeleton, the intersection point is the center of an inner bitangent circle. The osculating circle associated with the cusp contains the bitangent circle and, therefore, cannot lie inside the curve. Assume now that the segment does not cross the skeleton and consider the point of tangency between the osculating circle centered in the cusp and the curve. The radius of the circle is equal to or less then the radius of the bitangent circle associated with the point of tangency. The osculating circle has a high-order inner contact with the curve and, therefore, is a maximal circle fitted inside the curve. Thus its center, the cusp, lies on the skeleton. An inner bitangent circle of a generic closed curve has a high-order contact with the curve if and only if the circle center is a skeleton endpoint. Thus the cusp is an endpoint of the skeleton. This completes the proof.

The above theorem implies the following result describing dynamical properties of the skeleton of a figure evolving in time.

2D Skeleton Branching Theorem. For a simple closed curve evolving in time, consider the motion of an evolute cusp which lies inside the curve and points towards the curve (i.e., corresponds to a positive maximum of the curvature, if the curve is oriented by its inner normal). Assume that the cusp is moving toward the curve and the segment connecting the cusp and its associated curve point intersects the skeleton at one point only. When the cusp crosses the skeleton, a new branch of the skeleton is born with its endpoint at the cusp.

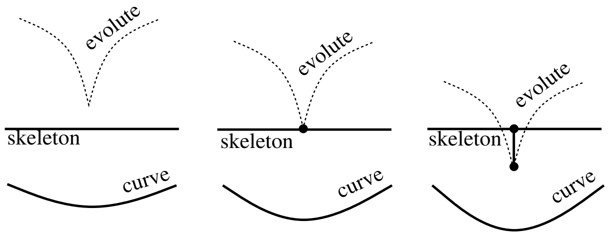

Fig. 7 visualizes the 2D Skeleton Branching Theorem.

3D Skeleton Branching Theorem

Focal surface. Consider a smooth generic surface. Denote by $k_{\max}$ and $k_{\min}$ the largest and the smallest principal curvatures, respectively, $k_{\max} \geq k_{\min}$. The principal centers of curvature are the points situated on the surface normals at the distances $1/k_{\max}$ and $1/k_{\min}$ from the surface. The loci of the principal centers from the focal surface. The focal surface consists of two sheets corresponding to the maximal and minimal principal curvatures.

The focal surface is the 3D analog of the evolute and has singularities. The singularities of the focal surface consists of space curves called the *focal ribs*. Near a point of a focal rib the focal surface can be locally represented in the parametric form $(c_1 t^3, c_2 t^2, s)$, where $c_1 \neq 0 \neq c_2$, in proper (curvilinear) coordinates (s, t). See Fig. 8 for a typical focal rib.

The focal ribs themselves may have singularities.

The surface curves corresponding to the focal ribs are natural generalization of the curve vertices for surfaces.

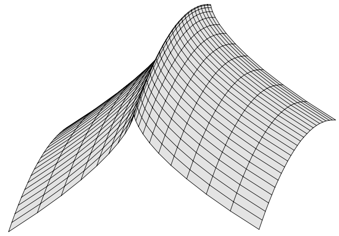

Figure 8. A typical focal rib.

For a surface given parametrically $\mathbf{r} = \mathbf{r}(u, v)$, its focal surface is described by:

$$\mathbf{f}(u, v) = \mathbf{r}(u, v) + \frac{\mathbf{n}(u, v)}{k(u, v)}, \qquad k = k_{\max}, k_{\min}, \quad (3)$$

where $\mathbf{n}(u, v)$ is the oriented normal (without loss of generality, we do not consider parabolic points in (3)).

Let at a point P on the surface the coordinates u, v be chosen so that the tangent vectors $\partial\mathbf{r}/\partial u$ and $\partial\mathbf{r}/\partial v$ coincide with the principal directions $\mathbf{t}_{\max}$ and $\mathbf{t}_{\min}$. If P corresponds to a singular point on the focal surface, then the cross product

$$\frac{\partial \mathbf{f}}{\partial u} \times \frac{\partial \mathbf{f}}{\partial v} = \\ = \frac{\partial \mathbf{r}}{\partial u} \frac{\partial k}{\partial u} \frac{k - k_{\min}}{k^3} + \frac{\partial \mathbf{r}}{\partial v} \frac{\partial k}{\partial v} \frac{k - k_{\max}}{k^3}$$

vanishes when k is either $k_{\max}$ or $k_{\min}$. This proves the following statement

Proposition 5 *For a smooth generic surface the singularities of the focal surface (focal ribs) correspond to the lines on the surface where either principal curvature has extrema along its associated principal direction and the points where the principal curvatures are equal (umbilics).*

See also [10] where a different proof of the above proposition is given.

Following [8] let us call the surface curves corresponding to the focal ribs the *principal curvature extremum curves*.

Skeleton. Consider a 3D figure F bounded by a piecewise-smooth closed surface ∂F. The skeleton of F is the closure of the set of points inside F that have more than one closest point among the points of ∂F.

One can define the skeleton of F as the locus of centers of maximal balls: balls inside F that are not themselves enclosed in any other ball inside F.

Various elements of the skeleton of a figure are shown schematically in Fig. 9 (we use the terminology accepted in [11] and [13]).

The *skeletal edge* of the skeleton of a figure is a connected space curve consisting of the skeletal points whose

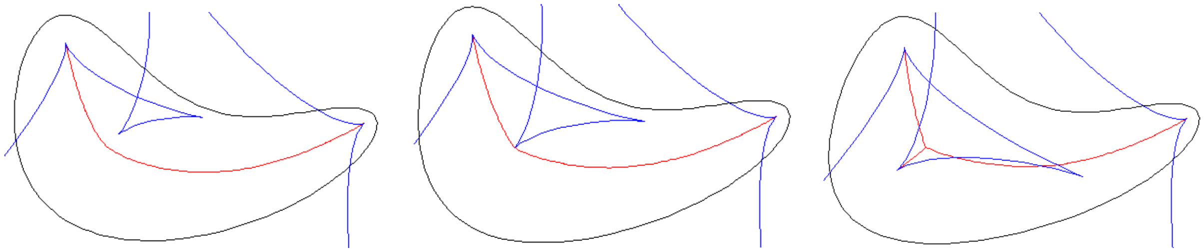

Figure 7. A curve, its evolute, and skeleton. Left: the skeleton is a curvilinear segment with two its endpoints located at evolute cusps; the evolute cusp pointing towards the skeleton does not serve as a skeleton endpoint. Middle: the cusp touches the skeleton. Right: when the cusp intersects the skeleton and a new skeleton branch with its endpoint at the cusp appears. Note that another evolute cusp does not give a birth to a skeleton branch when it intersects the skeleton because the segment connected that cusp and its associated curve vertex intersects the skeleton.

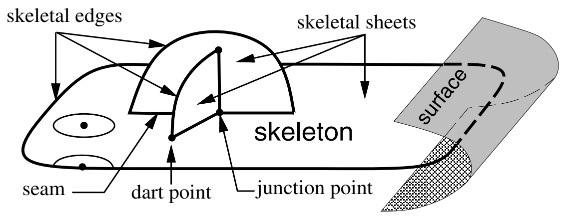

Figure 9.

small neighborhoods on the skeleton are topologically equivalent to a half-disk. One can also describe the skeletal edge points as the points whose maximal spheres have a single contact with the surface bounding the figure. A *skeletal sheet* is a connected component of the skeletal points whose small neighborhoods on the skeleton are topologically equivalent to a disk. A *seam point* is a skeletal point whose small neighborhood on the skeleton is topologically equivalent to a disc sewn with a half-disk. A *dart point* is a skeletal point whose small neighborhood on the skeleton is topologically equivalent to a disc sewn with a quarter-disk. A *junction point* is a skeletal point whose small neighborhood on the skeleton is topologically equivalent to a disc sewn with three quarter-disks. See Fig. 9.

For a smooth oriented surface, let us define the *ridges* as the loci of the positive maxima of the maximal principal curvature along its curvature line.

Relations between the skeletal edges, the ridges, and certain focal ribs are described by the following proposition (see [3], [2], and [4, Appendix]).

Proposition 6 *Consider a bounded 3D figure F whose boundary, ∂F, is smooth and oriented by its inner normal. The skeletal edges form a proper subset of those focal ribs associated with the maximal principal curvature which are pointing towards ∂F. Those ribs correspond to the ridges on ∂F.*

These relations between the ridges, the focal ribs associated with $k_{\max}$ and pointing towards the surface, and the skeletal edges are demonstrated schematically in Fig. 10 and for an elliptic paraboloid in Fig. 11.

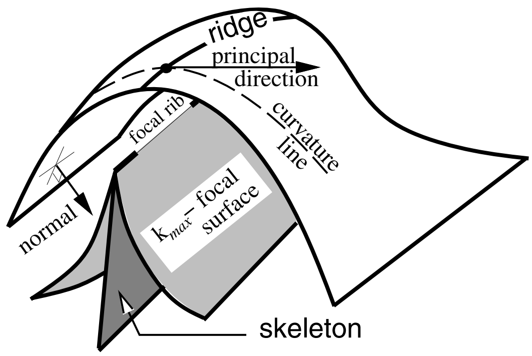

Figure 10. Relations between the focal ribs, curvature lines, and ridges are shown schematically.

A proof of Proposition 6 is sketched in the following three subsections.

Ridges. Consider a smooth surface. For a given non-umbilic point P on the surface let us choose coordinates in the space so that P is at the origin, the (x, y)-plane is the tangent plane to the surface at P, the principal directions $\mathbf{t}_{\max}$ and $\mathbf{t}_{\min}$ coincide with x and y axes, respectively, and the normal $\mathbf{n}$ coincides with z-axis. Then the surface is expressible in the Monge form as the graph of a generic

IEEE COMPUTER SOCIETY

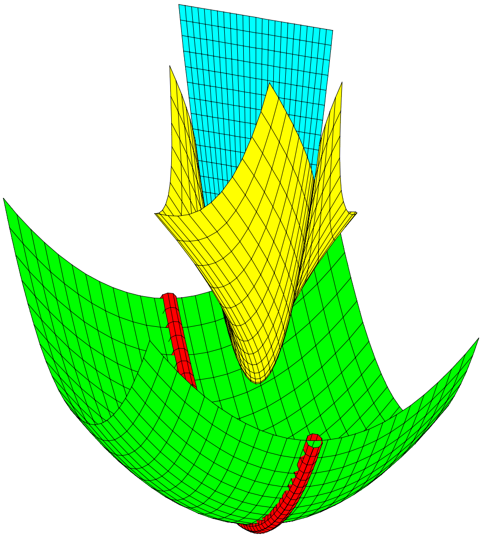

Figure 11. A surface (grey), a ridge on the surface (dark grey), the focal surface sheet associated with $k_{\max}$ (light grey), and the skeleton of the figure bounded by the surface (grey).

smooth function $z = F(x, y)$, where

$$F(x,y) = \frac{1}{2}\left(\lambda x^2 + \mu y^2\right) + \frac{1}{6}\left(ax^3 + 3bx^2y + 3cxy^2 + \right. \\ \left. + dy^3\right) + \frac{1}{24}\left(ex^4 + 4fx^3y + \dots\right) + O(x,y)^5$$

with $\lambda = k_{\max}(0,0)$, $\mu = k_{\min}(0,0)$, $\lambda > \mu$. Let the surface orientation be chosen so that the maximal principal curvature is nonnegative at P: $\lambda \geq 0$.

Since the vectors $(1,0)$ and $(0,1)$ represent $\mathbf{t}_{\max}$ and $\mathbf{t}_{\min}$ at P, respectively, then

$$\frac{\partial k_{\max}}{\partial \mathbf{t}_{\max}}(0,0) = a \qquad \frac{\partial k_{\max}}{\partial \mathbf{t}_{\min}}(0,0) = b \tag{4}$$

Let $e_{\max} = \partial k_{\max}/\partial \mathbf{t}_{\max}$. The extrema of the maximal principal curvature along its curvature line are given in the implicit form by the zeros of $e_{\max}$.

The curvature line associated with $k_{\max}$ is locally described by the problem

$$\frac{dy}{dx} = \frac{bx + cy}{\lambda - \mu} + O(x,y)^2, \qquad y(0) = 0.$$

Therefore, $y'(0) = 0$, $y''(0) = b/(\lambda - \mu)$ and in a neighborhood of the origin the curvature line is approximated by the parabola

$$y = \frac{bx^2}{2(\lambda - \mu)}.$$

It allows to compute the Taylor series expansion of $k_{\max}$ at the origin along the associated curvature line

$$\lambda + ax + \left(-3\lambda^3 + e + \frac{3b^2}{\lambda - \mu}\right)\frac{x^2}{2} + O(x^3) \tag{5}$$

Analyzing asymptotic expansion (5) we obtain that P is a generic ridge point (the maximal principal curvature has a positive maximum along its curvature line) iff

$$\lambda > 0, \quad a = 0, \quad A = -3\lambda^3 + e + \frac{3b^2}{\lambda - \mu} < 0. \tag{6}$$

Note that

$$A = \frac{\partial e_{\max}}{\partial \mathbf{t}_{\max}}(0,0) = \frac{d^2 k_{\max}}{ds_{\max}^2}(0,0),$$

where $s_{\max}$ is the arclength of the curvature line associated with $k_{\max}$.

If P is a ridge point, the tangent direction to the ridge at P is given by $\{Ax + By = 0,\ z = 0\}$, where

$$B = \frac{\partial e_{\max}}{\partial \mathbf{t}_{\min}}(0,0) = f + \frac{3bc}{\lambda - \mu}.$$

Contact with osculating spheres. Consider the intersection curve between the surface and the plane $\{y = \alpha z\}$, where α is a parameter. The curve is locally described by the equation $y = \alpha\lambda x^2/2 + \dots$. The Taylor expansion of the curvature of the curve is the product of $\sqrt{1+\alpha^2}$ and

$$\lambda + ax + \left[-3\lambda^3(1+\alpha^2) + 3\lambda^2\mu\alpha^2 + \right. \\ \left. + 6b\lambda\alpha + e\right]\frac{x^2}{2} + O(x^3) \tag{7}$$

Thus, if the origin is a ridge point ($a = 0$), the type of the extremum of the curvature along the intersection curve is defined by the sign of

$$-3\lambda^3(1+\alpha^2) + 3\lambda^2\mu\alpha^2 + 6b\lambda\alpha + e.$$

This expression is a quadratic polynomial in α. The discriminant is given by

$$D = 3\lambda^2(\lambda - \mu)A,$$

where A is defined in (6). The discriminant is negative if and only if the maximal principal curvature has a maximum along the intersection curve between the surface and the plane $\{y = \alpha z\}$ for any α. Now from (5) it follows that the osculating spheres (spheres of curvature) associated with $k_{\max}$ have inner contacts with the surface at the ridge points.

Fig. 12 shows the same surface, ridge, and focal sheet as in Fig. 11 and an osculating sphere touching the surface at a ridge point.

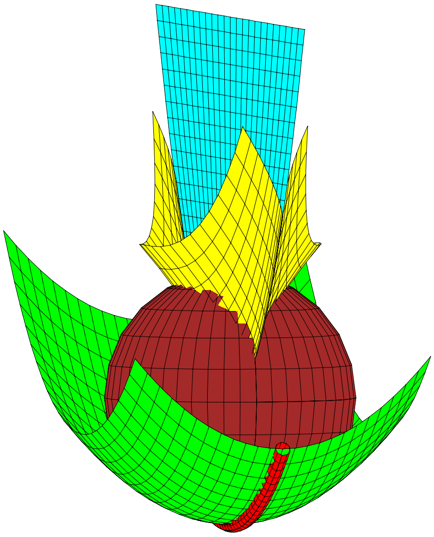

Figure 12. A surface (grey), a ridge on the surface (dark grey), the focal surface sheet associated with $k_{\max}$ (ligh t grey), the skeleton of the figure bounded by the surface (grey), an osculating sphere touching the surface at a ridge point (dark gray). The sphere has a single point contact with the surface.

Ridges and Focal Ribs. The intersection between the caustic sheet associated with $k_{\max}$ and the plane $\{y = 0\}$ gives a curve described locally by

$$x = -\frac{A}{3\lambda}t^3 + O(t^4), \quad z = \frac{1}{\lambda} - \frac{A}{2\lambda^2}t^2 + O(t^3).$$

At a neighborhood of the point $(0, 0, 1/\lambda)$ the intersection curve is locally a semicubical parabola. Thus the cuspidal edges (ribs) of the caustic sheet associated with $k_{\max}$ and pointing towards the surface correspond to the ridges.

3D Skeleton Branching Theorem. Consider a closed surface and a figure bounded by the surface. The skeletal edges of the skeleton of the figure are not necessarily located at focal ribs. If the sphere of curvature (osculating sphere) centered at a focal rib point does not lie inside the figure, then the point is not a skeletal edge point. Similarly to the 2D case we arrive at the following result.

Theorem 2 *Given a generic closed surface oriented by its inner normal, consider a point on a focal rib associated with the maximal principal curvature and pointing towards the surface (i.e., corresponding to a ridge). The point belongs to a skeletal edge if and only if the segment connecting the point and its associated ridge point does not cross the skeleton.*

We can reformulate this theorem to describe bifurcations of the skeleton of a figure evolving in time.

3D Skeleton Branching Theorem. Consider an evolving smooth closed surface oriented by its inner normal and a focal rib associated with the maximal principal curvature, pointing towards the surface (i.e., corresponding to a surface ridge). Let the rib touch and then intersect the skeleton during the surface evolution. Consider the rib point where the first contact between the skeleton and the rib occurs and the segment connecting the rib point and its associated surface point. Assume that the number of intersections between the segment and skeleton changes from one to zero during the evolution. Then a new skeletal sheet is born at the instant when the rib touches and intersects the skeleton.

Acknowledgments

We would like to thank the anonymous reviewers for their numerous constructive comments.

References

[1] J. August, A. Tannenbaum, and S. W. Zucker. On the evolution of the skeleton. In *Seventh International Conference on Computer Vision (ICCV'99)*, pages 315–322, 1999.

[2] A. G. Belyaev, E. V. Anoshkina, and T. L. Kunii. Ridges, ravines, and singularities. In A. T. Fomenko, and T. L. Kunii, *Topological Modeling for Visualization.* Ch. 18, pages 375–383, Springer, 1997.

[3] A. G. Belyaev, I. A. Bogaevski, and T. L. Kunii. Ridges and ravines on a surface and segmentation of range images. In *Vision Geometry VI, Proc. SPIE 3168*, pages 106–114, 1997.

[4] A. G. Belyaev and Y. Ohtake. An image processing approach to detection of ridges and ravines on polygonal surfaces. In A. de Sousa and J. C. Torres, editors, *Eurographics 2000, Short Presentations*, pages 19–28, August 2000.

[5] H. Blum. A transformation for extracting new descriptors of shape. In W. Wathen-Dunn, editor, *Symposium on Models for the Perception of Speech and Visual Form*, pages 362–380. MIT Press, 1967.

[6] H. Blum. Biological shape and visual science. *J. Theor. Biology*, 38:205–287, 1973.

[7] J. W. Bruce and P. J. Giblin. *Curves and Singularities : A geometrical introduction to singularity theory*. Cambridge University Press, 1992.

[8] M. Hosaka. *Modeling of Curves and Surfaces in CAD/CAM*. Springer, Berlin, 1992.

[9] D. Mumford. Mathematical theories of shape: Do they model perception. In B. C. Vemuri, editor, *Geometric Methods in Computer Vision, Proc. SPIE 1570*, 1991.

[10] I. R. Porteous. *Geometric Differentiation for the Intelligence of Curves and Surfaces*. Cambridge University Press, Cambridge, 1994.

[11] E. C. Sherbrooke, N. M. Patrikalakis, and E. Brisson. Computation of the medial axis transform of 3-d polyhedra. In C. M. Hoffman and J. Rossignac, editors, *Proceedings of the Third Symposium on Solid Modeling and Applications*, pages 187–199. ACM Press, 1995.

[12] D. J. Struik. *Lectures on Classical Differential Geometry*. Dover, 1988.

[13] G. M. Turkiyyah, D. W. Storti, M. Ganter, H. Chen, and M. Vimawala. An acceleration triangulation method for computing the skeletons of free-form solid models. *Computer-Aided Design*, 29(1):5–19, 1997.

[14] S. Yoshizawa and A. G. Belyaev. Visualization and study of dynamic 2d shapes via curvature. In *International Conference on Multimedia Modeling (MMM 2000)*, pages 469–489, Nagano, Japan, November 2000.

0-7695-0853-7/01 $10.00 © 2001 **IEEE**